Remote Sensing in Ecology and Conservation
Open Access
ZSL LET'S WORK FOR WILDLIFE

ORIGINAL RESEARCH

Observing ecosystems with lightweight, rapid-scanning terrestrial lidar scanners

Ian Paynter[1], Edward Saenz[1], Daniel Genest[1], Francesco Peri[1], Angela Erb[1], Zhan Li[1], Kara Wiggin[1], Jasmine Muir[2], Pasi Raumonen[3], Erica Skye Schaaf[4], Alan Strahler[5] & Crystal Schaaf[1]

[1]School for the Environment, University of Massachusetts Boston, Boston, Massachusetts
[2]Department of Science, Information Technology and Innovation, Queensland, Brisbane, Australia
[3]Department of Mathematics, Tampere University of Technology, Tampere, Finland
[4]Department of Geography, McGill University, Quebec, Montreal, Canada
[5]Department of Earth and Environment, Boston University, Boston, Massachusetts

Keywords
Compact biomass lidar (CBL), ecosystem properties, lidar, quantitative structure models, terrestrial lidar scanners, validation

Correspondence
Ian Paynter, School for the Environment, University of Massachusetts Boston, 100 Morrissey T. Blvd, Boston, MA 02125.
Tel: 617 287 7440; Fax: 617 287 7474;
E-mail: ian.paynter@umb.edu

Funding Information
We also acknowledge financial support from the Oracle Graduate Fellowship, the NASA Harriet Jenkins Graduate Fellowship, the UMass Boston International Research Initiative Seed Grants Program, and NASA grants NNX14AK12G and NNX14AI73G.

Editor: Harini Nagendra
Associate Editor: Doreen Boyd

Received: 30 May 2016; Revised: 2 July 2016; Accepted: 29 July 2016

doi: 10.1002/rse2.26

Abstract

A new wave of terrestrial lidar scanners, optimized for rapid scanning and portability, such as the Compact Biomass Lidar (CBL), enable and improve observations of structure across a range of important ecosystems. We performed studies with the CBL in temperate and tropical forests, caves, salt marshes and coastal areas subject to erosion. By facilitating additional scanning points, and therefore view angles, this new class of terrestrial lidar alters observation coverage within samples, potentially reducing uncertainty in estimates of ecosystem properties. The CBL has proved competent at reconstructing trees and mangrove roots using the same cylinder-based Quantitative Structure Models commonly utilized for data from more capable instruments (Raumonen et al. 2013). For tropical trees with morphologies that challenge standard reconstruction techniques, such as the buttressed roots of *Ceiba* trees and the multiple stems of strangler figs, the CBL was able to provide the versatility and the speed of deployment needed to fully characterize their unique features. For geomorphological features, the deployment flexibility of the CBL enabled sampling from optimal view-angles, including from a novel suspension system for sampling salt marsh creeks. Overall, the practical aspects of these instruments, which improve deployment logistics, and therefore data acquisition rate, are shown to be emerging capabilities, greatly increasing the potential for observation, particularly in highly temporally dynamic, inaccessible and geometrically complex ecosystems. In order to better analyze information quality across these diverse and challenging ecosystems, we also provide a novel and much-needed conceptual framework, the microstate model, to characterize and mitigate uncertainties in terrestrial lidar observations.

Introduction

Light detection and ranging (lidar) instruments are rapidly developing to provide robust estimates of important ecosystem properties at new spatial and temporal scales. Uncertainty in these estimates arises from characteristics of the instrument, complexities of the ecosystem and weather conditions during sampling. We provide a new conceptual framework, the *microstate model*, to establish these uncertainties. Through the application of the microstate model to a series of data-driven case studies of diverse ecosystems, we explore the unique advantages that these newly emerging rapid-scanning and lightweight lidar instruments may offer for reliably observing ecosystems.

Lidar instruments emit pulses of light energy. These pulses are reflected from objects, and lidar instruments record the time-of-flight and intensity of the returning

energy. This process provides information about the three-dimensional structure of an object or environment. Since many aspects of an ecosystem's condition are manifest in properties of its structure, lidar can monitor the condition of ecosystems through observations of their structure. As a result, lidar data are increasingly being used to augment and refine traditional passive remote sensing in the accurate assessment and reliable monitoring of ecosystems (Tang et al. 2014).

Lidar observations can be made at a range of spatial and temporal scales (Dubayah and Drake 2000; Lefsky et al. 2002; Hurtt et al. 2004; Zhao et al. 2012; Wulder et al. 2012), and from a variety of platforms (Lovell et al. 2003; Pfeifer and Briese 2007; Zolkos et al. 2013; Lucas et al. 2015; Woodhouse et al. 2011). This study focuses on terrestrial lidars, which typically scan their surroundings from a fixed point, using rotating mirrors and rotary stages to emit pulses in the surrounding directions. Terrestrial lidars have proven particularly useful for observing ecosystem structural properties in fine detail. This characterization of near-surface variation has established terrestrial lidars as important validation tools for airborne and satellite observations (Tang et al. 2014), as well as tools capable of producing independent observations of ecosystem structural properties.

At the present time, terrestrial lidar scanners are developing iteratively along two parallel pathways, which can be loosely termed *capability* and *practicality*. Capability is characterized by improvements in the attributes of individual lidar pulses, such as range, resolution and emitted wavelengths, increasing the maximum capabilities of an instrument. Contemporary archetypes include the research instruments, the Dual-Wavelength Echidna Lidar (DWEL) (Strahler et al. 2008; Douglas et al. 2012; Howe et al. 2015; Li et al. 2016) and the SALford Advanced Canopy Analyzer (SALCA) (Danson et al. 2014), and commercially available instruments such as the Riegl VZ-400 (Calders et al. 2015). While some of these highly capable instruments allow for variable scanning settings to decrease resolution and increase scanning speed, small, practical terrestrial lidar instruments offer the means to augment and extend the extensive, high-caliber information acquired with more capable scanners. Therefore, in this context, practicality is characterized by refinement, generally in the form of miniaturization and efficiency, to produce instruments that are lighter, faster and more resilient. Prominent examples include the research Compact Biomass Lidar (CBL) used in this study, and the commercially available Zebedee (Bosse et al. 2012) In the context of terrestrial lidar used for ecological investigation, the practical attributes of acquisition speed, portability and resilience can in themselves be considered important capabilities, necessary to properly characterize aspects of complex ecosystems.

There are many uncertainties and challenges involved in making terrestrial lidar observations of ecosystems. Prominently, lidar observations of structure are restricted to line-of-sight, creating a challenge when assessing the structural properties of an ecosystem. Since constrained areas of ecosystems are typically used as samples, it is expected that these areas will be fully observed with detailed lidar acquisitions. Yet, the line-of-sight limitations of lidar mean that certain regions or objects within ecosystem samples will be occluded, and therefore will not be observed, resulting in an incomplete characterization of the sample.

Lidar observations are further complicated as terrestrial lidar information density is range-dependent (Côté et al. 2009, 2011; Dassot et al. 2011), due to the angular separation between emitted pulses, resulting in larger gaps between observations over distance. Additionally, the quality of captured information can also be range-dependent, since individual lidar beams diverge with distance, resulting in lower specificity and accuracy of object detection. This means that even observed regions of samples are unlikely to have equal density and quality of information.

In response to these problems, it is common to perform multiple terrestrial lidar scans within an ecosystem sample, thus increasing the density of observations and variety of view angles. However, even the most intensive scanning cannot guarantee complete observation of an ecosystem sample. Additionally, capturing more scans considerably increases observation time, challenging the ability of terrestrial lidar to capture a complete sample, especially in ecosystems with high levels of temporal variation. Therefore, a comprehensive systematic understanding of the challenges to terrestrial lidar observations of ecosystems is urgently needed, accompanied by practical approaches to quantifying and mitigating these challenges.

The microstate model: a framework for understanding uncertainty in terrestrial lidar observations

Terrestrial lidar observations of ecosystem samples are typically made to assess one or more properties of interest, such as the number or volume of trees, the volume of a creek, or the surface structure of an eroding bluff. To understand and help mitigate the uncertainties in such observations of properties of interest within ecosystem samples, we have developed a conceptual framework called the *microstate model* (Fig. 1). This framework contextualizes aspects of documented sampling uncertainties in remote sensing (Phinn 1998) particularly for lidar sampling of ecosystems, and provides the systematic relationships between these aspects.

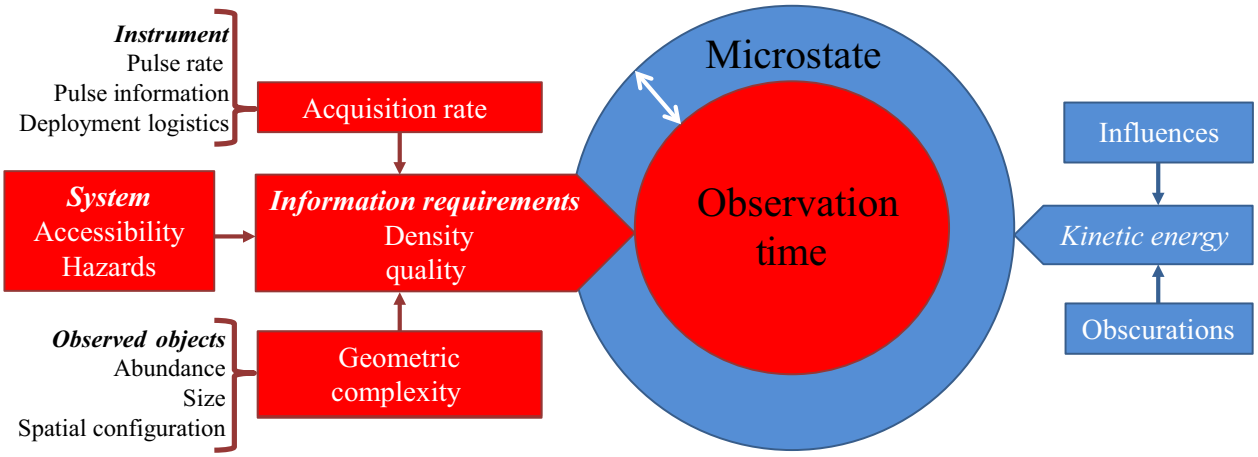

Figure 1. Conceptual diagram for the microstate model, designed to describe and provide a pathway to mitigate uncertainties and errors that arise from sampling ecosystem properties with lidar.

The microstate model comprises two major components. The first component describes how ecosystem temporal dynamism bounds the time available for sample observations. The second component concerns the propagation of error from individual lidar pulses, through interactions with ecosystem geometry, and ultimately to the uncertainty in an entire sample. Overall, the microstate model describes the requirements for terrestrial lidar observations of ecosystem samples to be appropriately constrained, complete and comparable.

Microstate model component 1: ecosystem temporal dynamism

Ecosystems are subjected to many temporally varying factors. These result from the import, export, movement or state change of matter within the ecosystem (Côté et al. 2009, 2011; Hancock et al. 2014). Intuitive examples arise from tidal cycles, seasonal influences, weather conditions, and other natural and anthropogenic disturbances. These temporal factors should be understood relative to the ecosystem properties of interest, such as tree height or creek volume. We can then categorize temporal factors as either obscurations of a property of interest, or influences upon it.

Influences are events that change the true value of a property of interest. They can take the form of import or export of relevant material from the sample space, or a state change of material within the sample space. *Obscurations,* on the other hand, are events that prevent, or increase uncertainty in, the observation of a property of interest, without changing its true value. One form of obscuration is the introduction of material to the sample space, such as a rising tide occluding geomorphological features. Obscurations can also be events that change the position of a terrestrial lidar relative to objects, or vice versa. Wind, for example, can alter the position of terrestrial lidars or the position of flexible objects such as tree branches during a scan, increasing uncertainty or preventing observation.

Appropriate observations of ecosystems can only be made during windows of time in which conditions are stable. Therefore, in the terminology just established, observations can only be made when obscurations and influences are absent. To define these stable spans of time, we can borrow the concept of 'microstate' from thermodynamics, where it refers to an instantaneous energetic state of a molecular-scale system (Hilser et al. 2006). A microstate in the context of ecosystems is a temporal window in which the ecosystem permits a discrete and accurate observation of a property of interest. By extension, observations made in equivalent microstates can be compared without concern. In practical terms, a microstate is the time *available* to complete an observation of one or more properties of interest of an ecosystem sample.

Microstate model component 2: sampling requirements

Lidar uncertainties originate at the pulse level, due to multiple factors which are dependent on the instrument's attributes and specifications. Primarily, uncertainties occur in the trajectory of an emitted pulse, and the range to an object, resulting in error between the observed and true position of a scattering object. Other sources of uncertainty include the shape and power of the outgoing pulse (Hosoi and Omasa 2007; Côté et al. 2009, 2011; Danson et al. 2014; Jupp et al. 2009); beam divergence; detector noise (Hancock et al. 2014; Douglas et al. 2015); and the precision of change detectable by the instrument.

Several of the factors that introduce uncertainty into each lidar pulse return can be range-dependent. This makes the uncertainty in ecosystem sampling partly dependent on the ecosystem's spatial properties and the geometry of objects in an ecosystem sample. An illustrative example is beam divergence, which is the increase in the width of a lidar beam with distance (Béland et al. 2014). Any interaction between an outgoing lidar pulse and an object is placed on the central trajectory of a pulse, which is inaccurate when an object only intersects a non-central portion of the beam. When lidar data are used to reconstruct objects, these misplaced returns can change the overall dimensions and other geometric properties of the objects, and this potential for positional error increases as the beam divergence increases with range.

The geometry and spatial configuration of objects in an ecosystem contribute greatly to the challenge of observing that ecosystem. The integration of the size, abundance, relative position and orientation of objects within the sample space of an ecosystem can be described as its *geometric complexity*. The geometric complexity of an ecosystem interacts with the line-of-sight nature of lidar to create inconsistent information gain and quality, causing the time required to observe an ecosystem sample to vary non-linearly with the overall size of the sample.

Additionally, to decide whether an ecosystem sample has been fully observed, we require a measurable threshold of the adequate terrestrial lidar information quantity and quality that must be met for each region and object in the sample for the sample to be considered valid. These thresholds can be collectively termed the *information requirements* for the sample. Appropriate values for information requirements would depend on the desired level of uncertainty in the final estimation of an ecosystem property. Preliminary experimentation, simulation or reference to similar studies can be used to suggest appropriate information requirements.

Different terrestrial lidars vary in the speed at which they can make observations of an ecosystem, according to their pulse rate and the space observed by each pulse. Also of importance are an instrument's deployment logistics, which are the time it takes to move and deploy the instrument. The combination of these factors gives each instrument an *acquisition rate*. The acquisition rate of an instrument, integrated with the information requirements of a study, and the geometric complexity of an ecosystem, determine an overall *observation time*. To summarize, the observation time is the time required to complete a valid observation of an ecosystem sample, while the microstate is the time available to complete an observation. If the observation time is shorter than the microstate, then the ecosystem sample can be validly observed (Fig. 1).

Materials and Methods

Hereafter, we describe several studies involving structural modeling of diverse ecosystems, conducted with terrestrial lidars optimized for acquisition speed, portability and resilience. These studies explore many challenges arising from the interactions described in the microstate model.

The terrestrial lidar data utilized for this study were provided by the first and second iterations of the CBL1 and CBL2 produced the by University of Massachusetts Boston (UMB) (Fig. 2). The instrument design is based on an initial concept by Katholieke Universiteit Leuven (Van der Zande et al. 2006), realized by the Rochester Institute of Technology (Kelbe et al. 2013, 2015) and extensively refined by UMB. The detailed specifications of the instruments are included in Figure 2. Note that the vertical angular resolution is the only data-relevant difference between the CBL1 and CBL2.

Unless otherwise stated, the instruments were deployed on a lightweight tripod such that the optical center was approximately 1.3 m above the ground. However, the light weight, compactness and resilience of the CBL provides immense flexibility for mounting the instrument on nontraditional platforms, such as tripods taller than 10 m, walk-up towers and overhead suspension systems. Where relevant, these are described below.

When multiple scans are acquired within a sample, these scans must be co-located (adjusted for relative position and rotation). For the CBL data in this study, an initial unsupervised co-location was performed when the relative location of scan positions was known. The final co-location of scans was supervised, involving visual assessment of common objects and features. Any returns not corresponding to the object of interest were manually removed.

Case Studies and Results

Norway maple

Trees are objects with extremely high geometric complexity, creating complex patterns of occlusion, and considerable uncertainty in their structural modeling with lidar. CBL2 scans were obtained at a distance of approximately 5 m in the four cardinal directions around a Norway maple (leaves on) in managed parkland in Boston, Massachusetts. Quantitative Structure Models (QSMs) for the tree were formed from the extracted tree points, using a reconstruction algorithm specifically designed for terrestrial lidar observations of trees (Raumonen et al. 2013; Kaasalainen et al. 2014; Krooks et al. 2014; Calders et al. 2015). The algorithm uses small point clusters to first segment the data into individual branches, and then fits a network of cylinders to the segmented data. Properties of

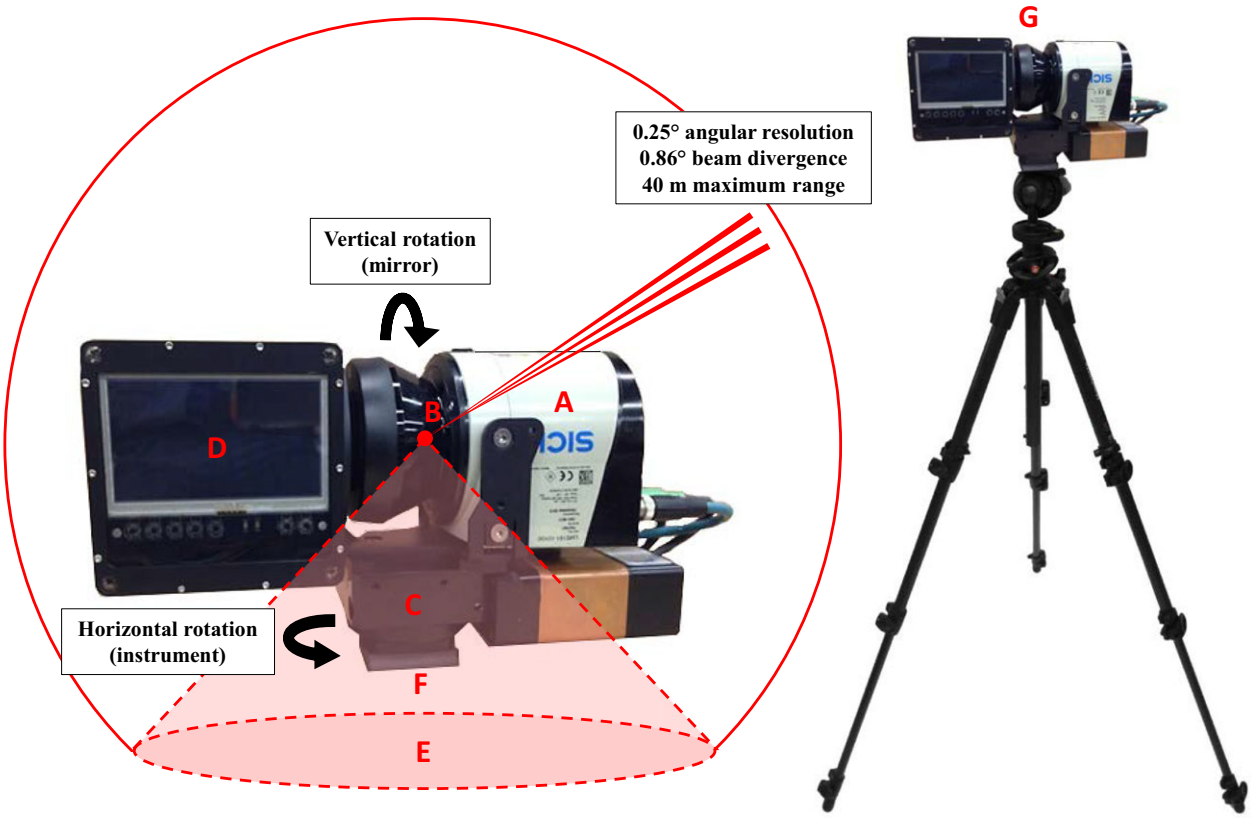

Figure 2. Compact Biomass Lidar 2 (CBL2) overall specifications: low weight (3.4 kg without tripod); small dimensions (40 cm × 15 cm × 25 cm); waterproof (IPv68); rapid scan time (33 sec); long battery life (1.5 h active use). (A) SICK LMS 151 Lidar unit: 905 nm wavelength; 40 m maximum range; 0.86° beam divergence; discrete returns (first and second); uncalibrated intensity. (B) Rotating mirror and detector: 0.25° vertical resolution (CBL1 0.5° vertical resolution). (C) Motor-driven rotary stage: 0.25°horizontal resolution; 360° horizontal view. (D) Beagle Bone Computer: Onboard data ingest; Onboard storage; Wireless control; Touchscreen control. (E) 270° vertical view (F) Flexible attachment for mounting on diverse platforms. (G) Mounted on tripod: 1.3 m optical center height.

the tree, including woody volume by branching order, can then be estimated using the geometric properties of the cylinders. The successful application of QSMs has been well-documented, particularly with highly capable terrestrial lidars (Calders et al. 2015; Raumonen et al. 2015). Since the clustering component of the algorithm involves random search patterns, 100 repeats of the reconstruction process were conducted with the CBL data (Fig. 3). The CBL produced reasonable and adequately stable volume estimates, which is encouraging given its considerable advantage in observation time, resulting from the instrument's high acquisition rate of 33 sec per scan (Fig. 2).

However, uncertainty in volume estimates between the QSM repeats, shown by the coefficient of variation, did notably increase with branching order (Table 1). This increased uncertainty could be attributed to several factors. Beam divergence creates range-dependent uncertainty in object position and geometry, which could translate into proportionally higher volume uncertainty in smaller objects such as the higher order branches, which are also generally farther from the terrestrial lidar when the instrument is deployed near ground-level. The information quantity and quality could also be decreased by occlusion from the lower order branches. Finally, although weather conditions were stable in this study, any obscuration by wind would have the greatest effect on the smaller, higher order branches, changing their position within and between scans, and increasing uncertainty.

Mangrove tree

Mangroves trees have exposed root systems, which increases their geometric complexity. Mangrove trees also reside in ecosystems with extremely high temporal dynamism, as tides can result in microstates of as little as 2 h

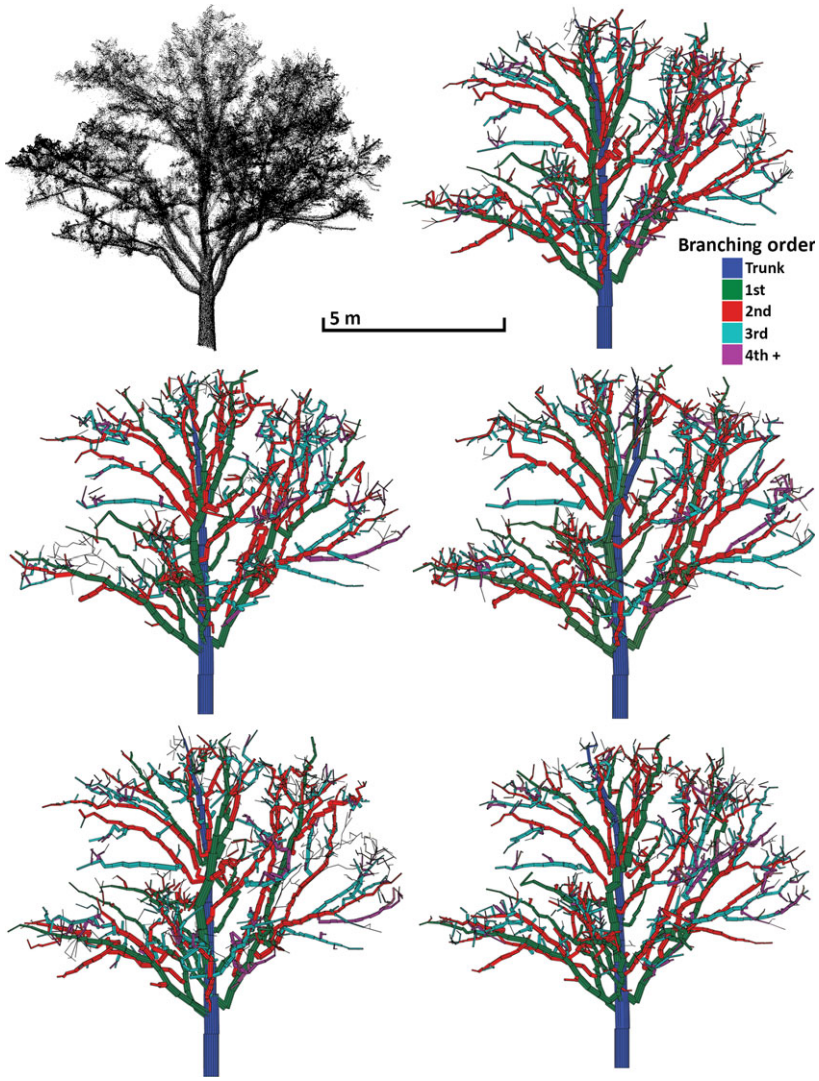

Figure 3. Point cloud (top left) of Norway Maple (Boston, MA), assembled from four CBL scans. The other panels are five Quantitative Structure Models (QSM). QSM reconstruction utilizes random selection of points during its clustering analysis, which creates variation between individual models, even while parameters remain the same. While some small differences between these cylinder models are visible, the overall structural consistency, and the quality of the representation of the point cloud are encouraging. Based on preliminary experimentation, QSM was utilized without filtering and parameterized as follows: d1 = 0.2; r1 = 0.22; n1 = 3; d2 = 0.05; r2 = 0.23; n2 = 3; l = 6; f = 0.5 (Raumonen et al. 2013, 2015). CBL, compact biomass lidar; QSM, quantitative structure models.

during which the full tree structure can be observed. In addition, mangroves are slow and hazardous to traverse, increasing observation time.

CBL1 scans were obtained of a 400 m^2 plot of red mangroves in Drake's Bay, Sarapiqui, Costa Rica, as part of a NASA EcoSAR (Rincon et al. 2011) field campaign. The plot was divided according to a 5 m × 5 m grid and scans were taken on the vertices of the grid. The entire 25 scan observation was conducted during a single low tide, leveraging the CBL's high acquisition rate (33 sec, 40 m range). For the reconstruction of the mangrove stem and root structure presented, the four closest scans were utilized. A QSM for the roots was reconstructed according to the principles used to reconstruct branches.

A hundred QSMs were successfully generated from the mangrove roots point cloud (Fig. 4), but higher coefficients of variation (Table 2) than in the Norway Maple tree (Table 1) suggested a higher overall uncertainty. This could be attributed to the need to adjust the parameterization of the QSM reconstruction algorithm when modeling roots, or that the CBL1's lower vertical (zenithal) resolution resulted in less certainty in object structure.

Deployment of terrestrial lidar in mangrove ecosystems has only previously been possible in areas with boardwalks (Knight et al. 2009; Kamal et al. 2015) or with deployment techniques that greatly increase observation time, such as scanning from a boat (Feliciano et al. 2014). The waterproofing of the CBL, coupled with its low weight, and favorable deployment logistics, enabled the observation of the particularly inaccessible mangroves in this study (Fig. 4).

Ceiba tree trunk

Tropical forest ecosystems have high geometric complexity at multiple scales. All trees are complex objects, but many tropical species have unique morphological features, such

Table 1. Volume estimates for the Norway Maple (Boston, MA) from QSMs.

	Mean (m^3)	S.D (m^3)	S.D/Mean (coeff. var.)
Total	3.766	0.153	0.041
Trunk	0.654	0.026	0.040
1st order branches	1.166	0.090	0.077
2nd order branches	1.153	0.093	0.081
3rd order branches	0.604	0.061	0.100
4th+ order branches	0.189	0.045	0.235

The mean, standard deviation and coefficient of variation (standard deviation divided by the mean) are presented for the 100 QSMs. Volumes are divided by branching order, with 1st order branches being those that are directly attached to the trunk, 2nd order directly branching off from 1st order, and so on. Note that the coefficient of variation increases through the branching orders, suggesting more variation between QSMs, and therefore higher uncertainty.

as buttressed roots, which further increase their geometric complexity. In addition, vertical stratification of vegetation, typically including dense understory, greatly increases occlusion and therefore observation time. CBL2 scans were obtained of the lower trunk of a large (approximately 40 m height) tree of the genus *Ceiba* within a Carbono study site (Clark and Clark 2000) at La Selva Biological Research Station (Sarapiqui, Costa Rica, 2014). Six scans were taken consecutively, at an approximate distance of 4 m from the tree center and at intervals of approximately 60°. An additional scan was taken inside a large hollow at the base of the trunk at an optical center height of 0.4 m. Observing atypical morphological features such as this hollow could improve non-destructive volume estimates for trees.

The outside of the trunk was captured with (Fig. 5) little apparent occlusion. The high acquisition rate of the CBL facilitated the observation of the many view angles necessary to fully capture the complex structure of the base of the *Ceiba* tree including its characteristic buttressed roots. The internal hollow occupied a substantial proportion of the tree base, and was a convoluted structure (Fig. 5). The compactness of the CBL, as well as the flexibility of its deployment platform, enabled the observation of this geometrically complex region of the object, which could impact volume, and therefore biomass, estimates from airborne and forestry measures.

There were still localized missing portions of the external and internal structure due to occlusion (Fig. 5). These could have easily been observed during the deployment with additional scans, given the high acquisition rate of the CBL. However, recognizing the need for additional scans would have required that information gain be characterized between scans, allowing iterative assessment of the occlusion.

Strangler fig tree

In addition to the previously described geometric complexity inherent to tropical forest ecosystems, strangler fig trees consist of many closely grouped stems, which are impossible to fully observe with lidar from the perimeter of the tree. CBL1 scans were obtained of a large, free-standing strangler fig in Corcovado National Park (Costa Rica, 2014) (Fig. 6) as part of a NASA EcoSAR (Rincon et al. 2011) field campaign. Scans were taken at intervals of approximately 12° around the strangler fig center (totaling 30 scans). Four additional scans were taken in the most accessible locations between the stems of the tree. Scanning between the stems of the strangler fig was only possible due to the compactness and portability of the CBL, and many structural components of the strangler fig were only captured by these internal scans (Fig. 7).

This study shows how the practical attributes of a terrestrial lidar can interact with the geometric complexity of an ecosystem sample. The scans taken around the strangler fig achieved higher information density in the lower regions of the tree (Fig. 7), even though the upper regions had a much greater extent. This suggests that internal regions of the canopy were occluded, which could be addressed in similar situations by deploying the CBL on a platform offering higher scanning positions. The lower vertical (zenithal) resolution of the CBL1 (0.5 degrees) compared to the CBL2 (0.25 degrees), and the range-dependent uncertainty resulting from beam divergence, may also contribute to the coarser definition of upper-canopy features.

Cave

Caves possess geometric complexity both in the form of large and frequently inaccessible occluded regions, and smaller features such as stalactites which contribute inter-object occlusion patterns similar to tree branches. CBL1 scans were obtained throughout a system of show-caves (Treak Cliff Caverns, Derbyshire, UK, 2014), for mapping. The scanning positions were determined ad hoc to maximize coverage, with consecutive scans in mutual line of sight (totaling 36 scans).

The favorable acquisition rate of the CBL permitted rapid capture of data throughout the entire cave system, providing excellent representation of the superstructure (Fig. 8). However, the resolution of the CBL1 limited its ability to characterize fine-scale structures such as stalactites. Higher resolution terrestrial lidar have proved capable of observing cave geomorphological structure in great detail (Hoffmeister et al. 2015; Mohammed Oludare and Pradhan 2016), and the Treak Cliff Caverns, which have constructed pathways, would certainly have been

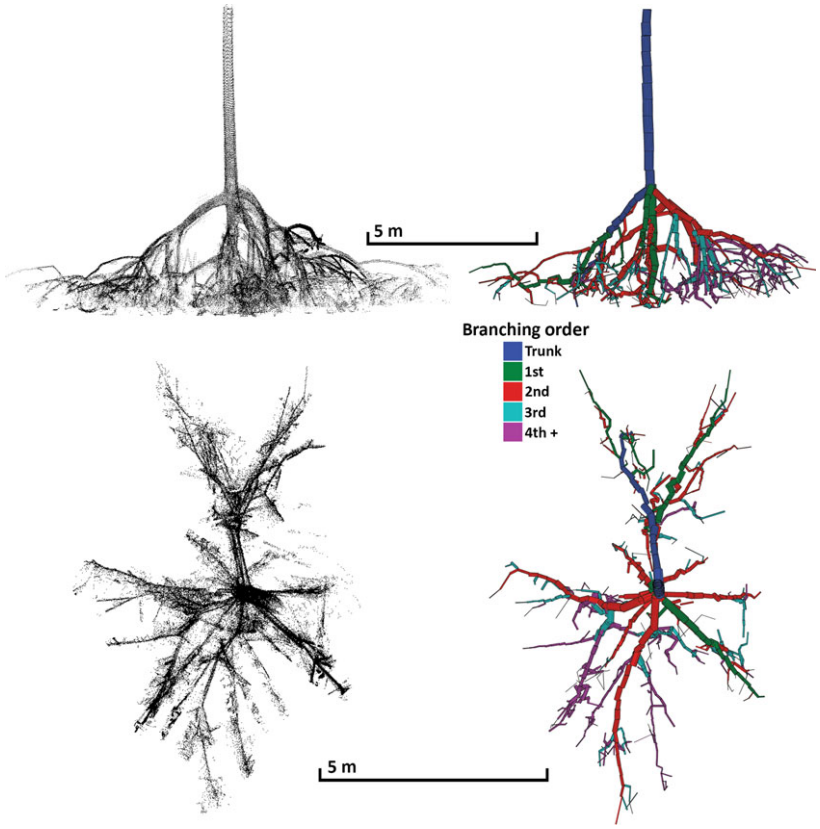

Figure 4. Point cloud (left) and QSM (right) of mangrove roots (Drake's Bay, Costa Rica). The cylinder model seems to represent the point cloud very well, even down to the fine roots. The overhead view (bottom) suggests that the four scans captured information to a reasonably high density with little residual occlusion. QSMs were reconstructed without filtering and parameterized as follows: d1 = 0.2; r1 = 0.22; n1 = 3; d2 = 0.05; r2 = 0.23; n2 = 3; l = 6; f = 0.5 (Raumonen et al. 2013, 2015). QSM, quantitative structure models.

Table 2. Volume estimates for mangrove tree roots from QSM.

	Mean (m^3)	S.D. (m^3)	S.D./Mean (coeff. var.)
Total	1.450	0.225	0.155
Trunk	0.465	0.054	0.115
1st order roots	0.363	0.144	0.396
2nd order roots	0.350	0.134	0.382
3rd order roots	0.183	0.059	0.328
4th+ order roots	0.088	0.056	0.632

The mean, standard deviation and coefficient of variation (standard deviation divided by the mean) are presented for 100 runs of QSM. Volumes are divided by root branching order, with 1st order branches being those roots that are directly attached to the trunk, 2nd order directly branching off from 1st order, and so on. Note that the coefficient of variation increases through the root branching orders, suggesting more variation between QSM runs, and therefore higher uncertainty. QSM, quantitative structure models.

accessible to larger, heavier instruments. However, for characterization of more inaccessible caves, or exploratory surveying where deployment flexibility is important, the CBL and similar practical instruments would offer considerable benefit. Utilizing platforms that provided a variety of scanning heights, as facilitated by the CBL's low weight, could also help mitigate occlusion resulting from cave geometric complexity.

Eroding bluff

Geomorphological features which are subject to erosion can have extremely high temporal dynamism during events such as storms. The low observation time and resilience of the CBL1 instrument enabled scanning within the short microstates and challenging conditions during a storm. Two CBL1 scans of an eroding bluff at Lovell's Island, Massachusetts, were obtained minutes apart during a storm event in April 2014 (Fig. 9). A third scan of the bluff was obtained by the CBL2 in January 2015. This dataset exemplifies influences on properties of interest, namely, the influence of wind and water on the position and shape of the bluff between time points (Fig. 10).

There was low magnitude, localized erosion observed in the minutes between scans during the storm in 2014, while erosion was widespread and of high magnitude across seasons, as revealed by the 2015 scan (Fig. 10). The bluff in 2015 was comparatively featureless, having fewer protrusions and indentations on its surface than in 2014 (Fig. 10).

These data also illuminate some considerations of information requirements. Gaps from a lack of information can be seen in the bluff data (Fig. 11), which could have been

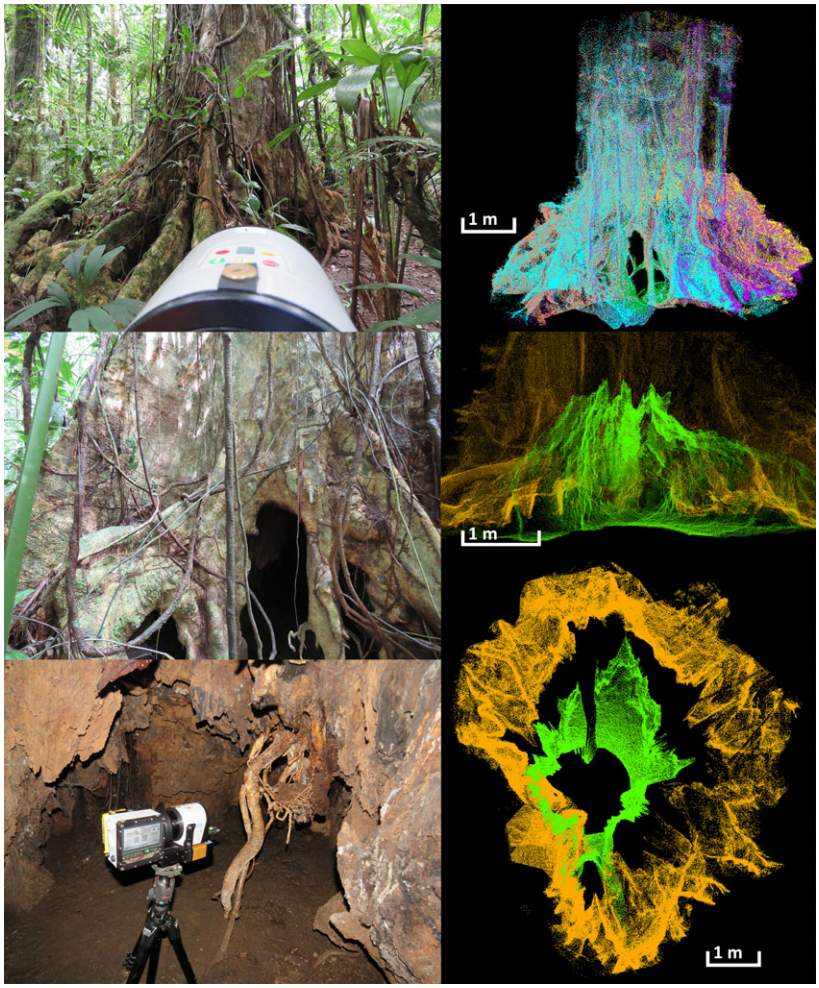

Figure 5. Photographs (left, top to bottom) of CBL2 scanning the exterior of the *Ceiba* tree (Costa Rica); the exterior of the hollow inside the trunk; and the CBL2 scanning the interior of the hollow. Point clouds (right, top to bottom) of the exterior of the *Ceiba* tree (colors denote source scans); structure from interior (green) and exterior (orange) CBL2 scans; and an overhead view of the trunk exterior (orange) and hollow interior (green). CBL, compact biomass lidar.

Figure 6. Photographs of the exterior (left) and interior with CBL1 (right) of the strangler fig (Costa Rica). The geometric complexity of the many separate stems created challenging patterns of occlusion that could only be mitigated by leveraging the compactness and rapid scanning of the CBL. CBL, compact biomass lidar.

precluded by establishing a required minimum information density. The importance of being able to monitor information gain during observation deployment is highlighted by the information density in the CBL2 observation at time point 3. More gaps would be expected in the lower density CBL1 data at time points 1 and 2. However, occlusion from a fallen tree in the foreground in the CBL2 data at time point 3 (Fig. 10) creates a locale of low information density (Fig. 11). This is also a clear example of the dependence of observations on the geometric complexity of the ecosystem sample.

Salt marsh creek

Salt marshes, like mangroves, are subject to tidal cycles that obscure observation of their geomorphological features and vegetation, and limit their accessibility. Microstates for salt marsh observation are typically very short, and vegetation growth or snow can also obscure geomorphology for large parts of the year. CBL2 scans were obtained of a tidal creek in the Plum Island Estuary, Massachusetts, Long Term Ecological Research (LTER) site, in 2015. The instrument was

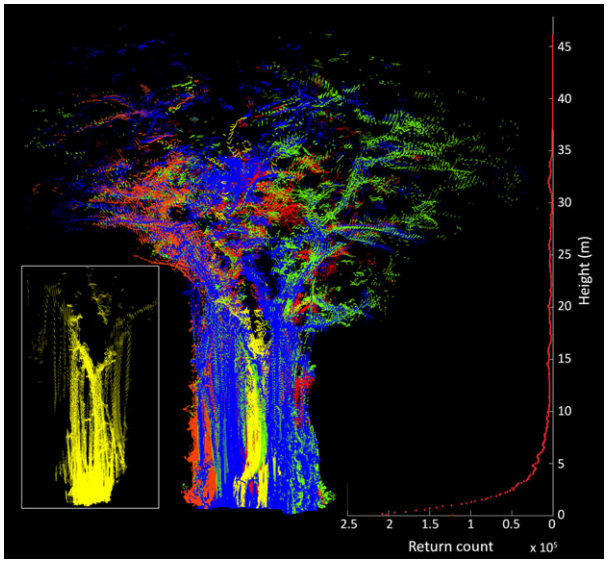

Figure 7. The point cloud (center) is colored according to contributions by external (red, green and blue) and internal (yellow) CBL1 scans. The unique structural features observed by the internal scans are also shown in isolation (left, yellow). The overall information density, in terms of the number of lidar returns, declined rapidly with height (right) due to the substantial occlusion of internal canopy structure, and angular separation between beams over the distance to the canopy of the tall tree. The strangler fig tree in this study completely collapsed during the following rainy season, with the CBL1 scans the only record of its structure. CBL, compact biomass lidar.

mounted upside down on a small tram, suspended above the creek by a cable tensioned by a pair of portable towers (Fig. 12). Five scans were taken at intervals of approximately 2 m along the creek.

The structure of the creek was captured with little occlusion, and reasonably even information density (Fig. 13). However, a raster analysis of the geomorphology (Fig. 14) shows some regions are still lacking information. Even though these regions are few in number and each less than 20 cm^2 in extent, these regions would still ideally have been observed. These data also demonstrate an additional obscuration which perturbed the scanner position. The effect of wind on the suspended scanner caused an accumulation of low magnitude ranging errors (Fig. 13). However, the optimal view angle for the ecosystem geometric complexity, achieved by mounting the lightweight and remotely operated CBL2 on a non-traditional suspended platform, greatly reduced occlusion and therefore observation time for the ecosystem sample.

It should be noted that the full absorption of lidar pulses by water in the bottom of the creek completely obscured observation of the underlying region. This is an illustrative application for the microstate model, since the extreme temporal dynamism of the salt marsh means that the microstates for observing creek geomorphology completely

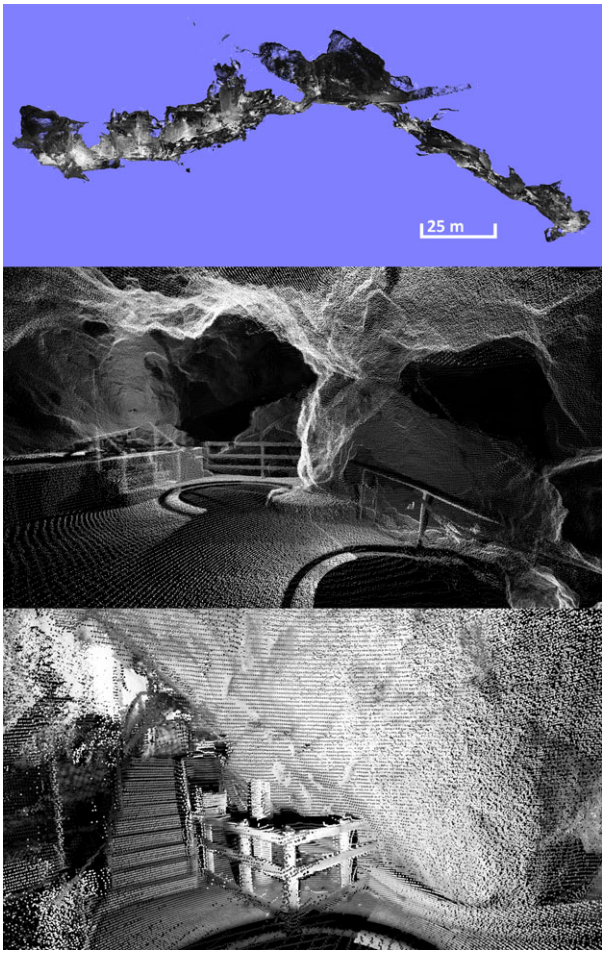

Figure 8. Point clouds of the complete structure of Treak Cliff Caverns (UK) (top); and particular regions (middle and bottom). The superstructure of the entire caverns were represented in the 36 CBL1 scans. However, there were some regions of occlusion, mostly associated with upward-facing surfaces, and variable information density, particularly in the taller caverns. CBL, compact biomass lidar.

may occur only briefly and at the lowest of low tides. The short observation time of the CBL and similar instruments, resulting from their acquisition rate and favorable deployment logistics, can meet the temporal constraints of such short microstates. Since vegetation growth and snow are additional obscuring factors for salt marsh creek geomorphology, observations are best made during late fall or early spring, facilitated by the wide operating temperature range, and IP68 waterproofing of the CBL.

Discussion

The trade-offs of practical terrestrial lidar scanners

These studies show how the practical attributes of terrestrial lidars such as speed, portability and resilience, are

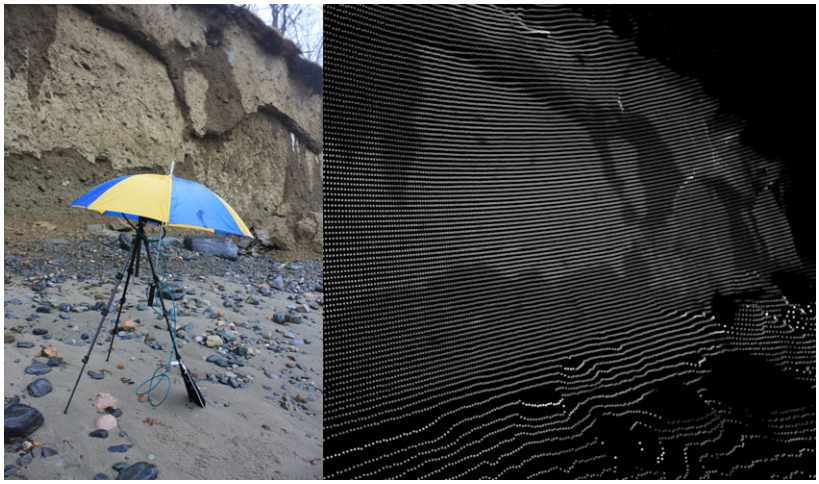

Figure 9. Photograph of eroding bluff on Lovell's Island (Boston, MA) (left) during April 2014 storm. CBL1 was covered with an umbrella between scans to protect from debris. The point cloud (right) shows the structural features of the bluff are clearly represented. The intensity (grayscale) of the CBL1 returns are sensitive to the varied water saturation of the bluff. CBL, compact biomass lidar.

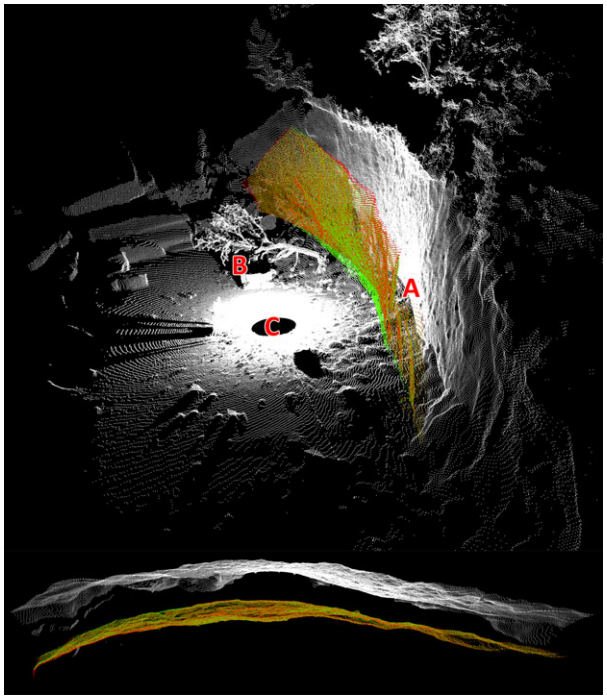

Figure 10. (Top) Extracted bluff sections of two scans taken minutes apart during April 2014 storm (red and green). These are overlaid on the full point cloud from January 2015 (white). (Bottom) Overhead view of extracted bluff sections for April 2014 (red and green) and January 2015 (white). Note the localized, minor erosion between the April 2014 scans, then the major erosion and retreat by January 2015 (A) including the deposition of a tree onto the beach (B). The footprint of the CBL scanning location can be seen (C). CBL, compact biomass lidar.

essential when observing properties of inaccessible, highly dynamic and geometrically complex ecosystems. Summarized in the terminology of the *microstate model*, low scan times and favorable deployment logistics improve the *acquisition rate* of practical terrestrial lidars, reducing *observation time*. Low weight, compactness and resilience help meet the accessibility challenges and hazards of ecosystems. Combined, these attributes enable fulfillment of *information requirements* even when sampling inaccessible ecosystems with high *geometric complexity* and short microstates.

There are trade-offs for these practicality optimizations, typically in the form of limitations to the quality and variety of information these instruments provide. Prominently, the angular resolution of the CBL is substantially lower than contemporary instruments such as the DWEL, SALCA and particularly the Riegl VZ-400, resulting in lower information density per scan. Additionally, the Riegl VZ-400 has a measurement range of up to 600 m, while the maximum range for the CBL is approximately only 40 m, meaning the CBL observes a much smaller space with each pulse.

These drawbacks are somewhat mitigated by the favorable deployment logistics of the CBL, enabling many scans to be taken from different locations within a sample, in the same time frame as a single scan from a higher resolution, longer range instrument. In fact, in *geometrically complex* environments such as tropical forests, the advantage of longer maximum range is reduced by the high degree of occlusion.

There are, however, still clear information benefits offered by highly capable commercial and research terrestrial lidars. For example, DWEL and SALCA use lasers of different wavelengths (1064 nm and 1548 nm) to separately identify returns from leaves and branches (Danson et al. 2014; Howe et al. 2015). More capable instruments such as DWEL, SALCA and Riegl may also record all or parts of the return waveform, at the very least providing more returns per pulse than the CBL, which only records the first and last. In addition, Riegl instruments utilize automatic co-alignment of scans based on deployed calibration targets, which add to deployment time, but

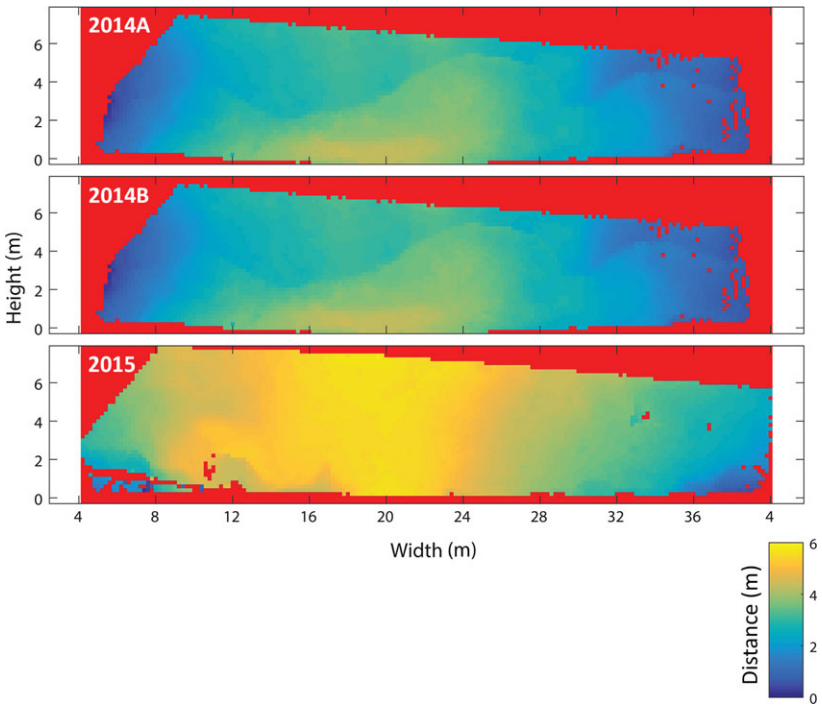

Figure 11. 20 cm rasters of extracted point clouds of bluff from CBL1 scans in April 2014 (top and middle) and January 2015 (bottom). Coloration denotes distance from plane intersecting scans position and parallel to bluff. Minor gaps (red) appear in areas further from the scanner, due to the lower information density with angular separation between beams over distance. These gaps are reduced slightly by the higher vertical resolution of the CBL2, utilized in January 2015 (bottom), but persist due to the increased distance to the retreating bluff, and the occlusion resulting from the fallen tree (Fig. 10, C). CBL, compact biomass lidar.

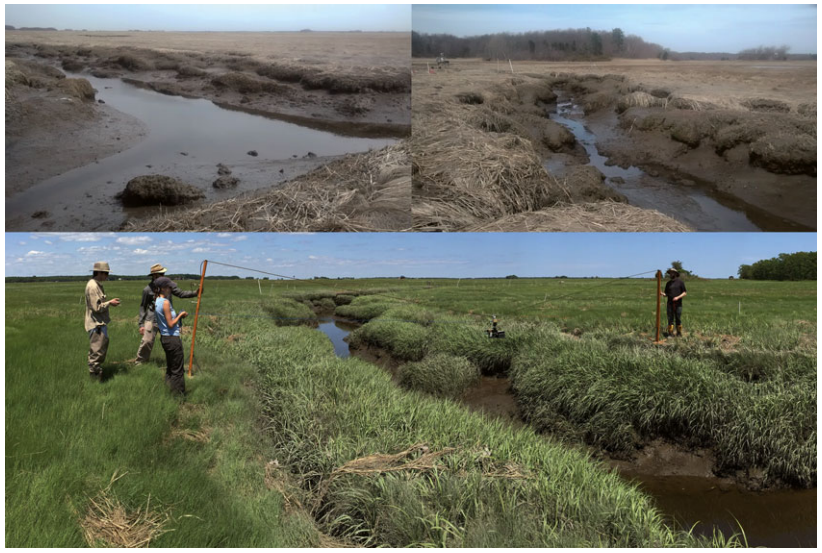

Figure 12. Photographs of salt marsh creeks at Plum Island (MA) (top) during winter months at low tide when vegetation and tide are not obscuring geomorphological features. The lightweight tower system for deploying CBL2 (bottom) is demonstrated during summer, when vegetation obscures creek banks. CBL, compact biomass lidar.

decreases post-processing time compared to the manual co-alignment of the CBL.

Furthermore, the CBL's beam divergence of 15 mrad (0.86 degrees), is substantially higher than that of most terrestrial lidars currently employed for ecosystem sampling, and even exceeds the angular resolution, creating overlap in the sampled volume. As previously mentioned, beam divergence can add considerable uncertainty to the bounds of objects, especially in small and finely clustered objects, such as higher order tree branches and leaves. Given the range-dependence of uncertainty from beam divergence, this uncertainty might be mitigated by filtering returns from beyond a certain range, and in tandem, setting information requirements to demand shorter range observations for all regions of the sample.

A final, essential context to this discussion is that the practical improvements in terrestrial lidars have been

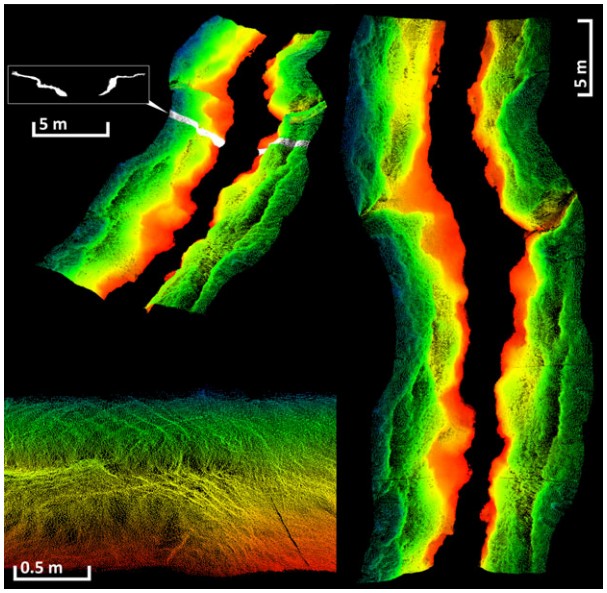

Figure 13. Point cloud of salt marsh creek from CBL2 scans (top left, colored by height), including extracted 20 cm profile (top, white and box). Creek point cloud viewed overhead (bottom left) and perpendicularly (bottom right). Note minor disagreements in bank structure (bottom right) resulting from wind influencing deployment platform during scans. Information density and representation of structure is excellent overall, with little evidence of occlusion. CBL, compact biomass lidar.

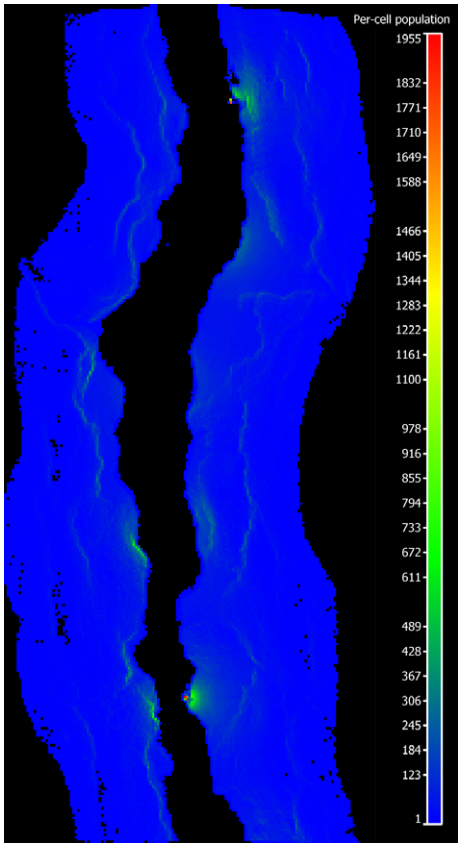

Figure 14. 10 cm raster image of return density for overhead view of salt marsh creek. Note the minor regions of missing information (black) within the bank structure, typically associated with upward facing surfaces and changes in elevation (Fig. 13).

accompanied by a notable reduction in cost. In addition, optimization of instruments such as the CBL for durability and resilience reduces the risk and therefore the functional cost of their deployment. Although financial cost is not a factor in the absolute scientific value of a method, it does influence information quality, since the cost of an observation method determines the spatial coverage achieved.

Evaluation of the microstate model

In these studies, the microstate model described the necessary conditions for observing diverse ecosystems. Using the microstate model, we were able to interpret the observations from each case study to suggest deficiencies and propose improvements. The microstate model responds dynamically to both the ecosystem-level factors, and changes to technologies and methodologies. For example, improvements in terrestrial lidar information quality or acquisition rate could enable observation of lower magnitude changes of an ecosystem property. This would, in turn, change the bounds of the microstate, as they are partly dependent on the possible resolution of observation.

The concept of information requirements provides an essential, measurable standard for terrestrial lidar observations. However, appropriate information requirements are specific both to an ecosystem property of interest and the method used to extract it from lidar data. Generally, information requirements for sampling will be derived from a desired maximum level of uncertainty in the downstream estimation of an ecosystem property. This is most easily achieved for problems with pre-existing data or the potential for simulation, but otherwise begets preliminary experimentation.

When determining observation time in the microstate model, it is useful to quantify a lidar's information quality. However, for spatially complex ecosystems, manufacturers' specifications may not accurately describe information quality. Therefore, independent calibration of instruments is recommended, utilizing objects with equivalent geometry and reflective properties to those found in the ecosystem to be sampled. Fortunately, pulse-level uncertainties can be robustly established with ever-improving methods (Kaasalainen et al. 2009; Li et al. 2016).

Dynamic sampling is a necessity and a challenge

Information requirements must be met for an observation to be considered complete. However, the unique geometry of each ecosystem sample means that the number and position of scans to meet information requirements will change. Therefore, a sampling design to meet information requirements cannot be predetermined. Instead, the necessary scan positions will have to be discovered during the observation of a sample, based on information gain reassessed after each scan. Additional scan positions can then be suggested based on accumulated information and projected information gain. This iterative process can be termed *dynamic sampling*.

Given that observations must be constrained to microstates, dynamic sampling methods must be very efficient, especially in ecosystems with high temporal dynamism. This presents a considerable computational challenge. However, ongoing work by the authors integrating improvements in lidar hardware and software with spatial algorithms places operational dynamic sampling close at hand.

Conclusions

Through the diverse studies presented herein, the practical attributes of terrestrial lidars are suggested to be true capabilities, establishing new potential possibilities in ecosystem sampling. The low weight and compactness of the Compact Biomass Lidar (CBL), and similar instruments, enable compatibility with diverse deployment platforms and greatly facilitate observations of geometrically complex ecosystems. This is particularly true in partitioned and stratified ecosystems such as tropical forests where the ability to mount terrestrial lidars on mobile towers allows scanning within occluded upper canopy regions. Utilizing such deployment platforms is only possible with remote instrument operation, which the CBL achieves through wireless control from mobile devices.

Improvements in lidar deployment logistics also enable the investigation of shorter microstates, as well as sampling in direct response to influential, episodic events such as storms. Combining these capabilities can even facilitate the partitioning of influential events into observable microstates. For example, we demonstrated the ability to observe erosion of a bluff within a storm (Fig. 12–14). This could lead to the coupling of specific erosion effects to specific and measurable components of the storm event.

Terrestrial lidars have shown great promise as validation tools for airborne and satellite estimations of ecosystem properties (Cook et al. 2009; Perroy et al. 2010; De Sy et al. 2012; Avitabile et al. 2016), and shorter observation times provide the ability to expand ecosystem sample volumes and increase information gain. These improvements in the validation capability of lidar instruments for diverse ecosystems is particularly timely with the Global Ecosystem Dynamics Investigation (GEDI) lidar scheduled to begin acquisitions from the International Space Station in 2018.

Ultimately, terrestrial lidar scanning is a rapidly developing technology, with a lot to offer to ecosystem analysis and monitoring. However, the potential of terrestrial lidar is utterly reliant on proper characterization and mitigation of its uncertainties, further development of upstream methods and protocols, and refinement and standardization of downstream processing and analysis techniques. We submit that lidar instruments optimized for practicality, coupled with the robust and adaptable conceptual framework of the microstate model may offer vital contributions toward these goals.

Acknowledgments

We gratefully acknowledge assistance from David and Deborah Clark, William Miranda, Leo Campos, Andres Vega, Temilola Fatoyinbo, Linda Deegan, Jack Payette, Jennifer Ly, and the Harrison and Turner families of Treak Cliff Caverns. We also acknowledge financial support from the Oracle Graduate Fellowship, the NASA Harriet Jenkins Graduate Fellowship, the UMass Boston International Research Initiative Seed Grants Program, and NASA grants NNX14AK12G and NNX14AI73G.

Data Accessibility

The large on-disk size of our lidar data limits our ability to submit the data for this paper to a public repository. However, we can host it indefinitely, with a publically accessible link, on the University of Massachusetts Boston data servers.

Conflict of Interest

None declared.

References

Avitabile, V., M. Herold, G. Heuvelink, S. L. Lewis, O. L. Phillips, G. P. Asner, et al. 2016. An integrated pan-tropical biomass map using multiple reference datasets. *Glob. Change Biol.* **22**,1406–1420.

Béland, M., D. D. Baldocchi, J. L. Widlowski, R. A. Fournier, and M. M. Verstraete. 2014. On seeing the wood from the

leaves and the role of voxel size in determining leaf area distribution of forests with terrestrial LiDAR. *Agric. For. Meteorol.* **184**, 82–97.

Bosse, M., R. Zlot, and P. Flick. 2012. Zebedee: design of a spring-mounted 3-D range sensor with application to mobile mapping. *Robotics*, IEEE Transactions on **28**, 1104–1119.

Calders, K., G. Newnham, A. Burt, S. Murphy, P. Raumonen, M. Herold, et al. 2015. Nondestructive estimates of above-ground biomass using terrestrial laser scanning. *Methods Ecol. Evol.* **6**, 198–208.

Clark, D. B., and D. A. Clark. 2000. Landscape-scale variation in forest structure and biomass in a tropical rain forest. *For. Ecol. Manage.* **137**, 185–198.

Cook, B. D., P. V. Bolstad, E. Næsset, R. S. Anderson, S. Garrigues, J. T. Morisette, et al. 2009. Using LiDAR and quickbird data to model plant production and quantify uncertainties associated with wetland detection and land cover generalizations. *Remote Sens. Environ.* **113**, 2366–2379.

Côté, J. F., J. L. Widlowski, R. A. Fournier, and M. M. Verstraete. 2009. The structural and radiative consistency of three-dimensional tree reconstructions from terrestrial lidar. *Remote Sens. Environ.* **113**, 1067–1081.

Côté, J. F., R. A. Fournier, and R. Egli. 2011. An architectural model of trees to estimate forest structural attributes using terrestrial LiDAR. *Environ. Model. Softw.* **26**, 761–777.

Danson, F. M., R. Gaulton, R. P. Armitage, M. Disney, O. Gunawan, P. Lewis, et al. 2014. Developing a dual-wavelength full-waveform terrestrial laser scanner to characterize forest canopy structure. *Agric. For. Meteorol.* **198**, 7–14.

Dassot, M., T. Constant, and M. Fournier. 2011. The use of terrestrial LiDAR technology in forest science: application fields, benefits and challenges. *Ann. For. Sci.* **68**, 959–974.

De Sy, V., M. Herold, F. Achard, G. P. Asner, A. Held, J. Kellndorfer, et al. 2012. Synergies of multiple remote sensing data sources for REDD+ monitoring. *Curr. Opin. Environ. Sustain.* **4**, 696–706.

Douglas, E. S., A. H. Strahler, J. Martel, T. Cook, C. Mendillo, R. Marshall, et al. 2012. DWEL: A Dual-Wavelength Echidna® Lidar for ground-based forest scanning, Proceedings IEEE International Geoscience and Remote Sensing Symposium 2012, Munich, Germany, **2012**, 5.

Douglas, E. S., J. Martel, Z. Li, G. Howe, K. Hewawasam, R. Marshall, et al. 2015. Finding leaves in the forest: the dual-wavelength echidna lidar. *Geosci. Remote Sens. Lett, IEEE* **12**, 776–780.

Dubayah, R. O., and J. B. Drake. 2000. Lidar remote sensing for forestry. *J. Forest.* **98**, 44–46.

Feliciano, E. A., S. Wdowinski, and M. D. Potts. 2014. Assessing mangrove above-ground biomass and structure using terrestrial laser scanning: a case study in the Everglades National Park. *Wetlands* **34**, 955–968.

Hancock, S., R. Essery, T. Reid, J. Carle, R. Baxter, N. Rutter, et al. 2014. Characterising forest gap fraction with terrestrial lidar and photography: an examination of relative limitations. *Agric. For. Meteorol.* **189**, 105–114.

Hilser, V. J., E. B. García-Moreno, T. G. Oas, G. Kapp, and S. T. Whitten. 2006. A statistical thermodynamic model of the protein ensemble. *Chem. Rev.* **106**, 1545–1558.

Hoffmeister, D. S., A. Zellmann, M. Pastoors, P. Kehl, J. Cantalejo, G. C. Ramos, et al. 2015. The investigation of the Ardales Cave, Spain–3D documentation, topographic analyses, and lighting simulations based on terrestrial laser scanning. *Archaeol. Prospec.* **23**, 75–86.

Hosoi, F., and K. Omasa. 2007. Factors contributing to accuracy in the estimation of the woody canopy leaf area density profile using 3D portable lidar imaging. *J. Exp. Bot.* **58**, 3463–3473.

Howe, G. A., K. Hewawasam, E. S. Douglas, J. Martel, Z. Li, A. Strahler, et al. 2015. Capabilities and performance of DWEL, the dual-wavelength echidna® lidar. *J. Appl. Remote Sens.* **9**, 13. doi:10.1117/1.JRS.9.095979.

Hurtt, G. C., R. Dubayah, J. Drake, P. R. Moorcroft, S. W. Pacala, J. B. Blair, et al. 2004. Beyond potential vegetation: combining lidar data and a height-structured model for carbon studies. *Ecol. Appl.* **14**, 873–883.

Jupp, D. L., D. S. Culvenor, J. L. Lovell, G. J. Newnham, A. H. Strahler, and C. E. Woodcock. 2009. Estimating forest LAI profiles and structural parameters using a ground-based laser called 'Echidna®. *Tree Physiol.* **29**, 171–181.

Kaasalainen, S., A. Krooks, A. Kukko, and H. Kaartinen. 2009. Radiometric calibration of terrestrial laser scanners with external reference targets.*Remote Sens.* **1**, 144–158.

Kaasalainen, S., A. Krooks, J. Liski, P. Raumonen, H. Kaartinen, M. Kaasalainen, et al. 2014. Change detection of tree biomass with terrestrial laser scanning and quantitative structure modelling. *Remote Sens.* **6**, 3906–3922.

Kamal, M., S. Phinn, and K. Johansen. 2015. Object-based approach for multi-scale mangrove composition mapping using multi-resolution image datasets. *Remote Sens.* **7**, 4753–4783.

Kelbe, D., P. Romanczyk, J. van Aardt, and K. Cawse-Nicholson. 2013. Reconstruction of 3D tree stem models from low-cost terrestrial laser scanner data. *SPIE Defense, Secur. Sens.* **8731**, 6.

Kelbe, D., J. van Aardt, P. Romanczyk, M. van Leeuwen, and K. Cawse-Nicholson. 2015. Single-scan stem reconstruction using low-resolution terrestrial laser scanner data. *IEEE J. Sel. Top Appl. Earth Observ. Remote Sens.* **8**, 3414–3427.

Knight, J. M., P. E. Dale, J. Spencer, and L. Griffin. 2009. Exploring LiDAR data for mapping the micro-topography and tidal hydro-dynamics of mangrove systems: an example from southeast Queensland, Australia. *Estuar. Coast. Shelf Sci.* **85**, 593–600.

Krooks, A., S. Kaasalainen, V. Kankare, M. Joensuu, P. Raumonen, and M. Kaasalainen. 2014. Predicting tree structure from tree height using terrestrial laser

scanning and quantitative structure models. *Silva Fenn.* **48**, 1125.

Lefsky, M. A., W. B. Cohen, G. G. Parker, and D. J. Harding. 2002. Lidar remote sensing for ecosystem studies lidar, an emerging remote sensing technology that directly measures the three-dimensional distribution of plant canopies, can accurately estimate vegetation structural attributes and should be of particular interest to forest, landscape, and global ecologists. *Bioscience* **52**, 19–30.

Li, Z., D. L. Jupp, A. H. Strahler, C. B. Schaaf, G. Howe, K. Hewawasam, et al. 2016. radiometric calibration of a dual-wavelength, full-waveform terrestrial lidar. *Sensors* **16**, 313.

Lovell, J. L., D. L. Jupp, D. S. Culvenor, and N. C. Coops. 2003. Using airborne and ground-based ranging lidar to measure canopy structure in Australian forests. *Canad. J. Remote Sens.* **29**, 607–622.

Lucas, R. M., A. L. Mitchell, and J. Armston. 2015. Measurement of forest above-ground biomass using active and passive remote sensing at large (subnational to global) scales. *Current Forest. Rep.* **1**, 162–177.

Mohammed Oludare, I., and B. Pradhan. 2016. A decade of modern cave surveying with terrestrial laser scanning: a review of sensors, method and application development. *Int. J. Speleol.* **45**, 8.

Perroy, R. L., B. Bookhagen, G. P. Asner, and O. A. Chadwick. 2010. Comparison of gully erosion estimates using airborne and ground-based LiDAR on Santa Cruz Island, California. *Geomorphology* **118**, 288–300.

Pfeifer, N., and C. Briese. 2007. Geometrical aspects of airborne laser scanning and terrestrial laser scanning. *International Archives of Photogrammetry, Remote Sensing and Spatial Information Sciences* **36** (3/W52), 311–319.

Phinn, S. R. 1998. A framework for selecting appropriate remotely sensed data dimensions for environmental monitoring and management. *Int. J. Remote Sens.* **19**, 3457–3463.

Raumonen, P., M. Kaasalainen, M. Åkerblom, S. Kaasalainen, H. Kaartinen, M. Vastaranta, et al. 2013. Fast automatic precision tree models from terrestrial laser scanner data. *Remote Sens.* **5**, 491–520.

Raumonen, P., E. Casella, K. Calders, S. Murphy, M. Åkerblom, and M. Kaasalainen. 2015. Massive-scale tree modelling from TLS data. *ISPRS Ann. Photogrammetry, Remote Sens. Spat. Inform. Sci.* **2**, 189.

Rincon, R. F., T. Fatoyinbo, G. Sun, K. J. Ranson, M. Perrine, M. Deshapnde, et al. 2011. The ECOSAR P-band Synthetic Aperture Radar. In 2011 IEEE International Geoscience and Remote Sensing Symposium.

Strahler, A. H., D. L. Jupp, C. E. Woodcock, C. B. Schaaf, T. Yao, F. Zhao, et al. 2008. Retrieval of forest structural parameters using a ground-based lidar instrument (Echidna®). *Canad. J. Remote Sens.* **34**(sup2), S426–S440.

Tang, H., M. Brolly, F. Zhao, A. H. Strahler, C. L. Schaaf, S. Ganguly, et al. 2014. Deriving and validating leaf area index (LAI) at multiple spatial scales through lidar remote sensing: a case study in Sierra National Forest, CA. *Remote Sens. Environ.* **143**, 131–141.

Van der Zande, D., W. Hoet, I. Jonckheere, J. van Aardt, and P. Coppin. 2006. Influence of measurement set-up of ground-based LiDAR for derivation of tree structure. *Agric. For. Meteorol.* **141**, 147–160.

Woodhouse, I. H., C. Nichol, P. Sinclair, J. Jack, F. Morsdorf, T. J. Malthus, et al. 2011. A multispectral canopy LiDAR demonstrator project. *IEEE Geosci. Remote Sens. Lett.* **8**, 839–843.

Wulder, M. A., J. C. White, R. F. Nelson, E. Næsset, H. O. Ørka, N. C. Coops, et al. 2012. Lidar sampling for large-area forest characterization: a review. *Remote Sens. Environ.* **121**, 196–209.

Zhao, F., A. H. Strahler, C. L. Schaaf, T. Yao, X. Yang, Z. Wang, et al. 2012. Measuring gap fraction, element clumping index and LAI in Sierra Forest stands using a full-waveform ground-based lidar. *Remote Sens. Environ.* **125**, 73–79.

Zolkos, S. G., S. J. Goetz, and R. Dubayah. 2013. A meta-analysis of terrestrial aboveground biomass estimation using lidar remote sensing. *Remote Sens. Environ.* **128**, 289–298.

